Theoretical investigation of contact-induced phenomena in composite materials containing fullerenes and nanotubes deposited on ferromagnetic substrates

Evgenia A. Kovaleva

Siberian Federal University

Krasnoyarsk, 2016

Aims of study

- to characterize the interactions of buckminsterfullerene C_{60}, CNTs or BNNTs with ferromagnetic transition metals, namely, Fe, Co and Ni, as well as half-metallic $La_{0.7}Sr_{0.3}MnO_3$
- to elucidate the nature of spin polarization of the nanosized fragments caused by interactions with ferromagnetic supports

Utilization of carbon and BN nanotubes for spintronic purposes

- Contact-induced spin polarization in graphene and h-BN on nickel and cobalt
- Graphene and h-BN as nanotubes of infinite diameter
- Finite thickness and curvature of CNT and BNNT influences the interface properties

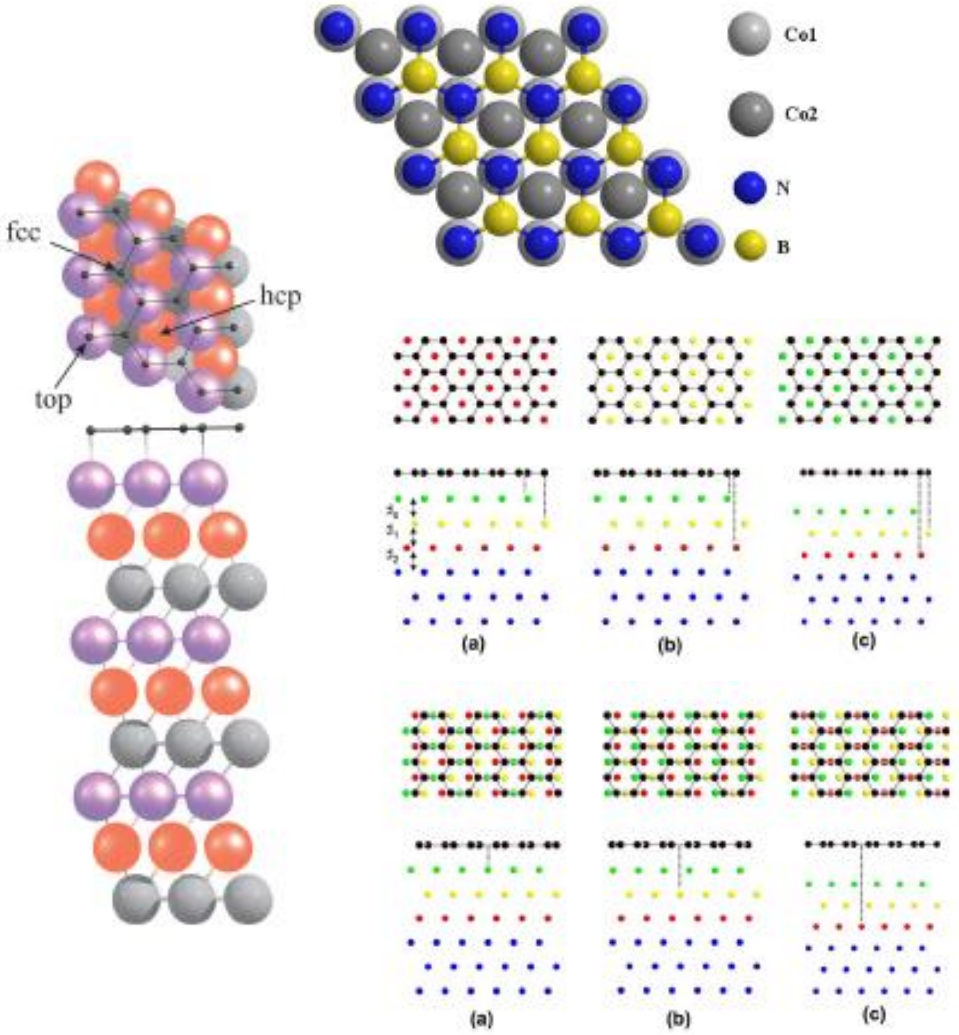

Organic spin valves

- Rubrene
- Pentacene
- Alq_3 (tris(8-hydroxyquinolino)aluminum)
- C_{60} is considered to be especially promising due to the absence of atoms other than carbon and, hence, weaker hyperfine interaction.
- Complex behavior combining GMR resulted from spin injection and TMR due to the presence of pinholes in organic spacer
- Aluminum oxide was found to suppress cobalt diffusion into the spacer layer effectively.
- Competition between positive GMR channel and pinhole channel

- The nature of interface between C_{60} and LSMO is relatively less investigated

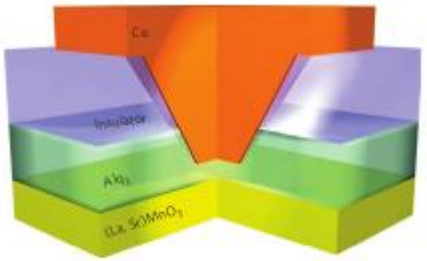

Figure 1 | Schematic drawing of the organic MTJ. The device consists first of a $La_{0.7}Sr_{0.3}MnO_3/Alq_3$ bilayer. A nanoindent in the Alq_3 layer is realized by a CT-AFM, allowing us to control the organic tunnel barrier thickness. This nanohole is then filled with cobalt, leading to a $La_{0.7}Sr_{0.3}MnO_3/Alq_3$/Co nanometric-size MTJ.

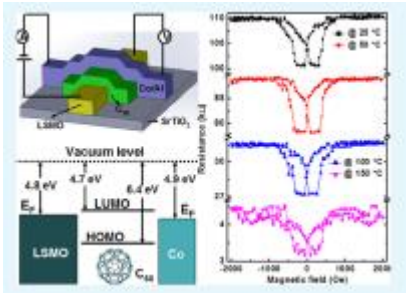

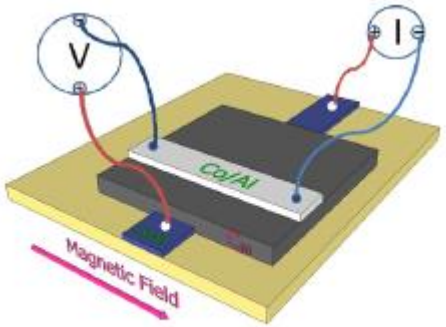

Fig. 1. Structure of LSMO/C_{60}/Co spin-valve and diagram of the 4-point measurement.

R. Lin et al., *Synth. Met.*, 2011, **161**, 553.
C. Barraud et al., *Nat. Phys.,* 2010, **6**, 615.
F. Li, *ACS Appl. Mater. Interfaces*, 2013, **5**, 8099.

Lanthanum strontium manganite $La_{0.7}Sr_{0.3}MnO_3$

- High Curie temperature (T_c=370K)
- Colossal magnetoresistance
- Half-metallicity
- High efficiency of spin injection
- Usage in spintronics, spin valves

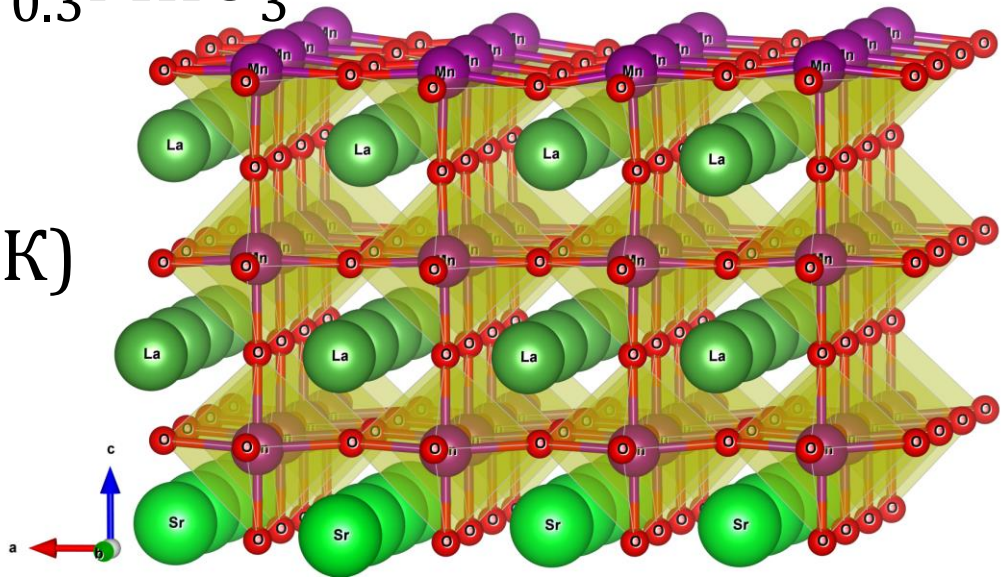

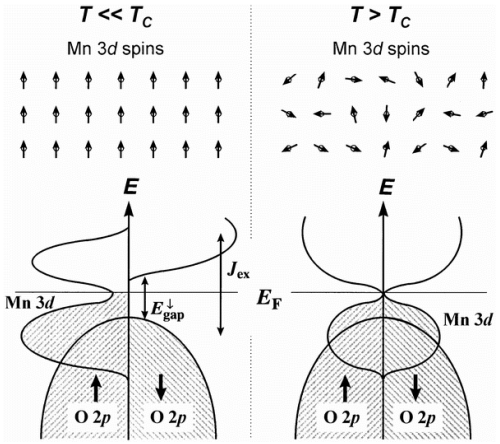

J.-H. Park et al. *Nature* **392**, 794-796 (1998)
doi:10.1038/33883

Computational methods

- Vienna Ab-initio Simulation Package
- Periodic boundary conditions
- LDA/GGA PBE
- Hubbard correction (GGA+U)
  - U=2 and J=0.7 for Mn in LSMO
    - C. Ma, Z. Yang, and S. Picozzi, *J. Phys. Condens. Matter*, 2006 **18**, 7717.
    - S. Picozzi, C. Ma, Z. Yang, R. Bertacco, M. Cantoni, A. Cattoni, D. Petti, S. Brivio, and F. Ciccacci, *Phys. Rev. B*, 2007, **75**, 94418.
    - B. Zheng and N. Binggeli, *Phys. Rev. B*, 2010, **82**, 245311.
- Grimme D3 correction for van-der-Waals interaction
- Plane wave basis set
- Ultrasoft pseudopotential/PAW method
- Bader charge analysis

Configurations of carbon and BN nanotubes on Co(0001) and Ni(111) slabs

(a,b) *top:fcc*; (c,d) *top:hcp*

(a) *top(N):hcp(B)*; (b) *top(N):fcc(B)*

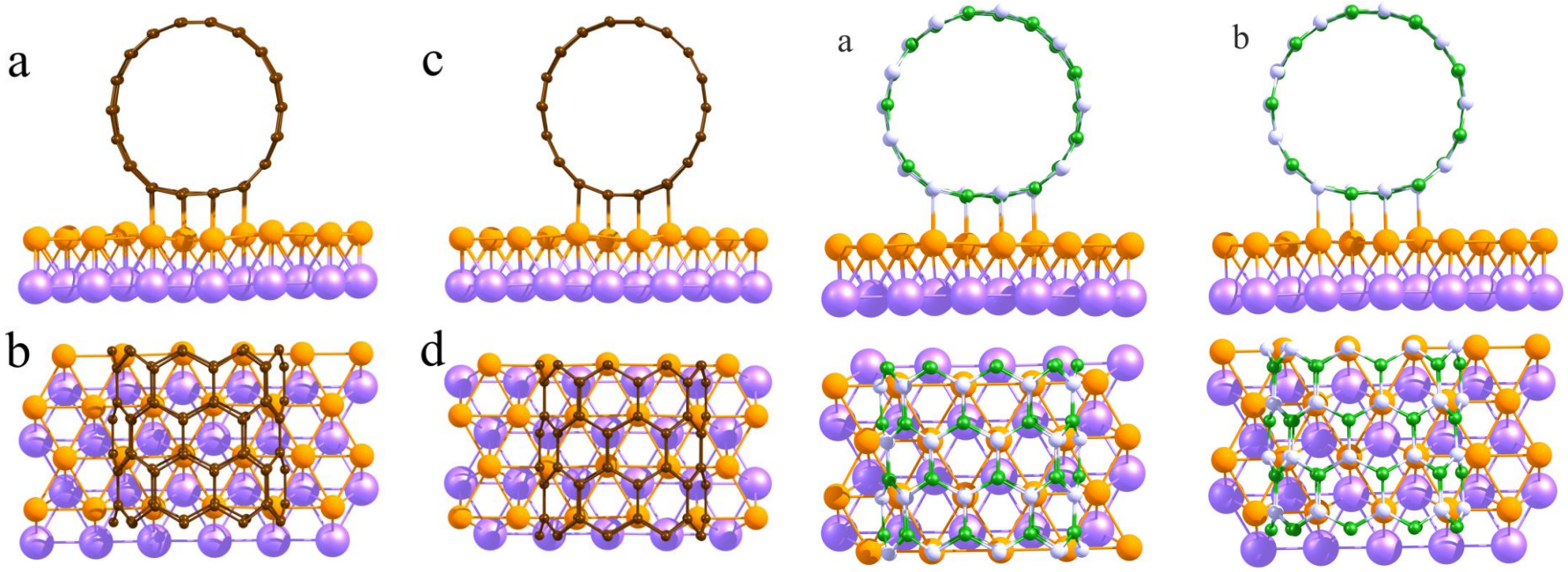

Nanotube	Metal	*top:fcc*	*top:hcp*
CNT(9,0)	Co	-4.646	-4.720
	Ni	-2.600	-2.374
CNT(10,0)	Co	-4.523	-4.360
	Ni	-2.260	-2.311
BNNT(9,0)	Co	-3.876	-3.926
	Ni	-1.891	-1.693

Substrate-induced conductivity in BNNT

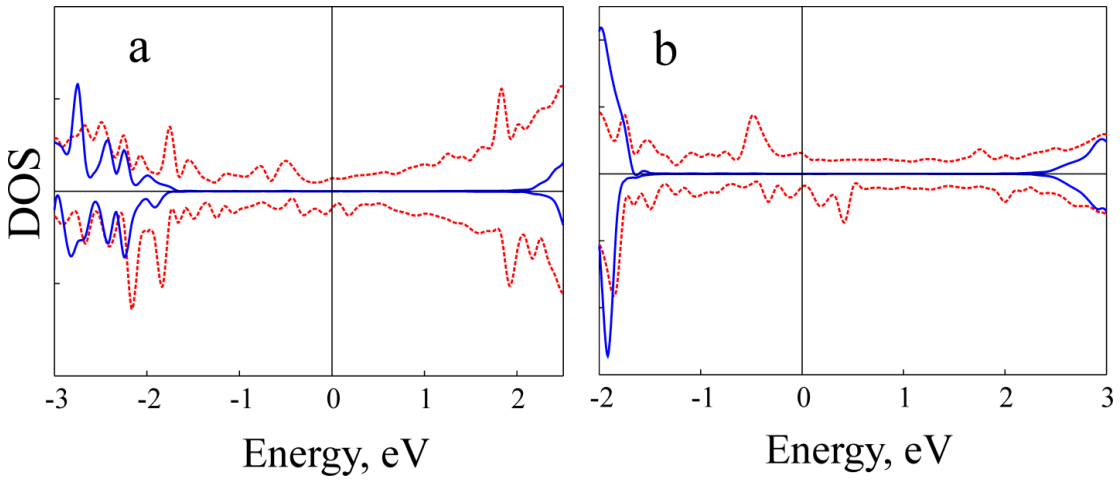

PDOS for B (a) and N (b) atoms in BNNT(5,5)/Ni system.

A.A. Kuzubov, E.A. Kovaleva, F.N. Tomilin, N.S. Mikhaleva, A.V. Kuklin, *Journal of Magnetism and Magnetic Materials,* 2015, **396**, 102–105.

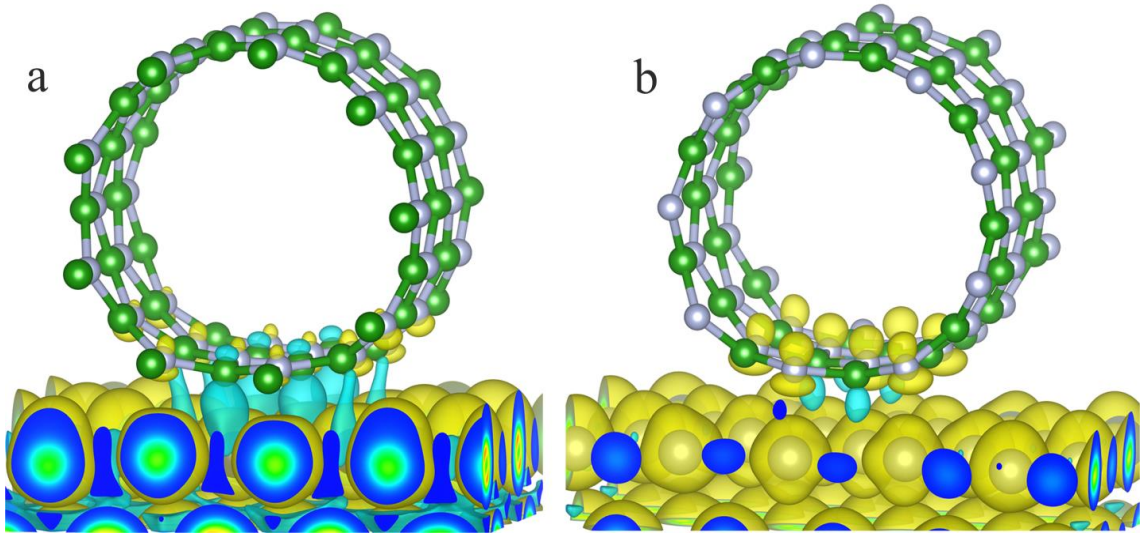

Spatial spin density distribution in BNNT(9,0)/Co (a) and BNNT(9,0)/Ni (b). Yellow and blue areas correspond to spin-up and spin-down density. Boron and nitrogen atoms are denoted as green and grey balls, respectively.

Carbon atoms PDOS (a,b) and spatial spin density distribution (c,d) in CNT(10,0)/Co (a,c) and CNT(10,0)/Ni (b,d) composites

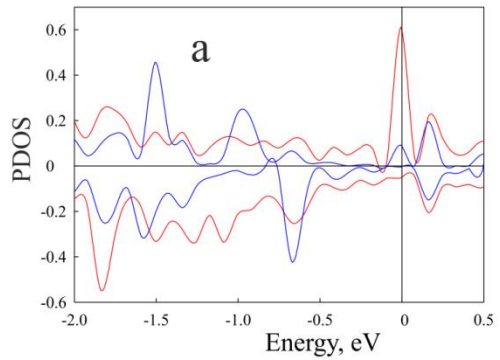

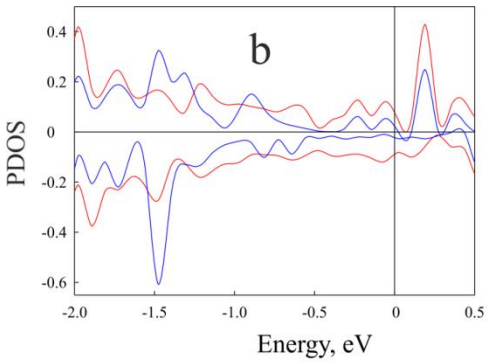

Isosurface level = 0,002 μ_B/ Å^3

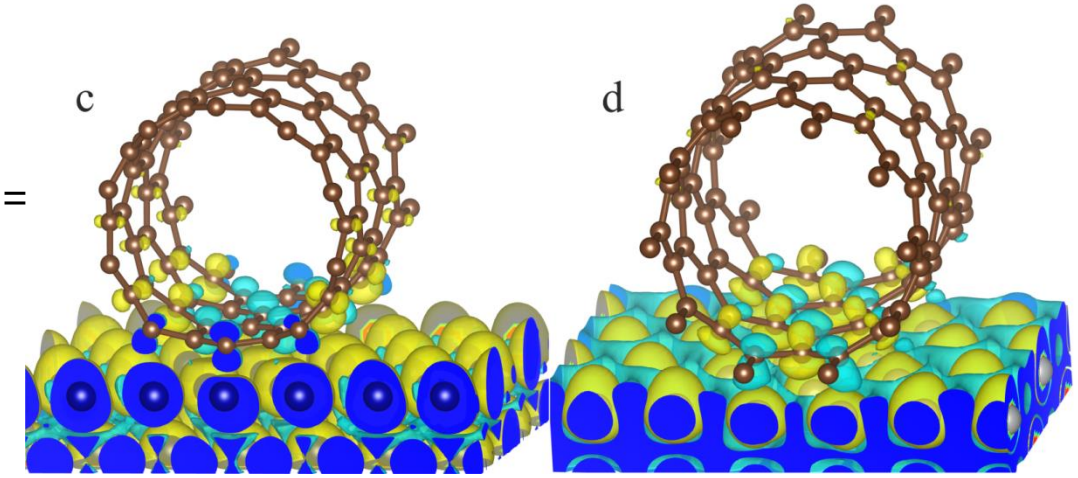

Isosurface level = 0,0008 μ_B/ Å^3

- a,b – PDOS for atoms in direct contact with metal and atoms far from the interface designated as red and blue lines, respectively
- c,d – yellow and blue areas correspond to spin-up and spin-down density

A.A. Kuzubov, E.A. Kovaleva, P. Avramov, A.V. Kuklin, N.S. Mikhaleva, F.N. Tomilin, S. Sakai, S. Entani, Y. Matsumoto, H. Naramoto, *Journal of Applied Physics*, 2014, **116**, 084309.

Optimized structures of C_{60}/Fe(100) nanocomposites

$$\xi = \frac{n_\uparrow - n_\downarrow}{n_\uparrow + n_\downarrow}$$

Configuration	Binding energy, eV	Charge, e	Magnetic moment, μ_B	Spin polarization at E_F, %
bridge-1	-3,082	2,217 (94,0)	-0,124	-72,6
bridge-2	-3,274	2,112 (95,5)	-0,153	38,3
2C-bond	-2,945	1,904 (86,7)	-0,040	-28,2
4C-atop	-2,921	1,667 (81,6)	-0,153	51,7

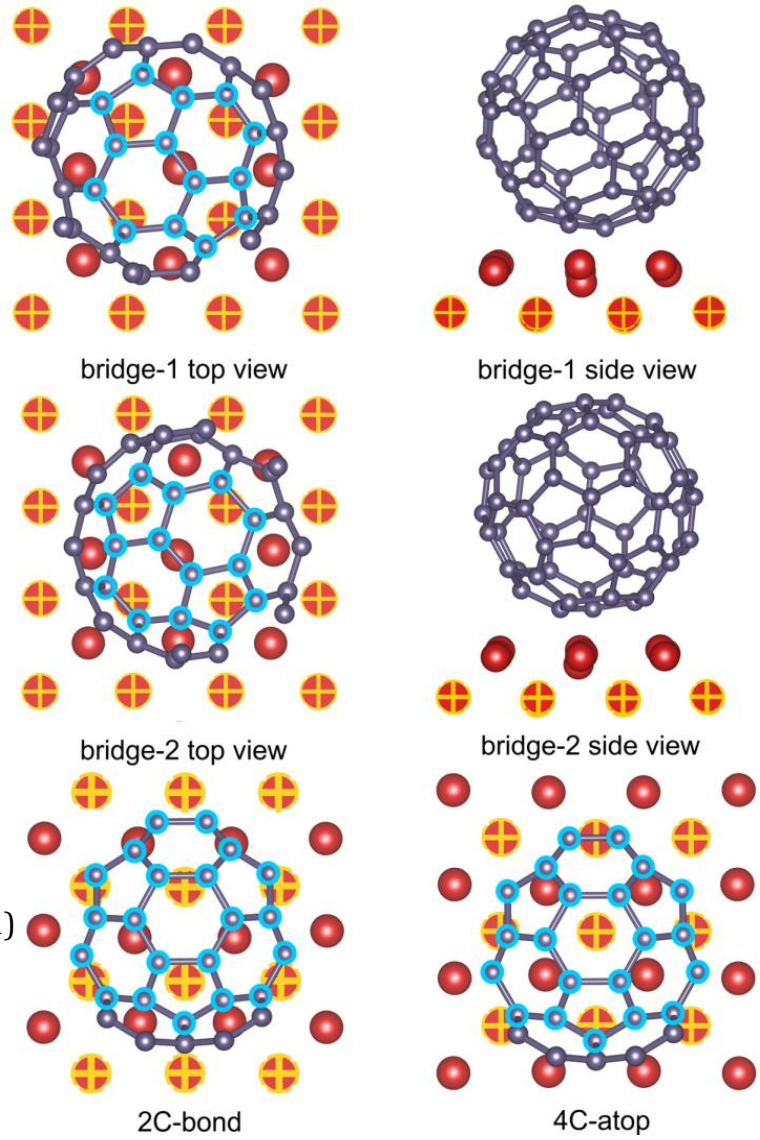

E_b = -2,9 эВ (Tran et al. *ACS Appl. Mater. Interfaces,* 2013, **5**, 837−841)

E_b = -3,06 эВ (Yang et al. *J. Phys. Chem. C*, 2015, **119**, 10532−10537)

A.A. Kuzubov, E.A. Kovaleva, P.V. Avramov, A.S. Kholtobina, N.S. Mikhaleva, A.V. Kuklin, *Journal of Magnetism and Magnetic Materials*, 2016, **410**, 41-46.

Substrate-induced changes in C_{60} electronic structure

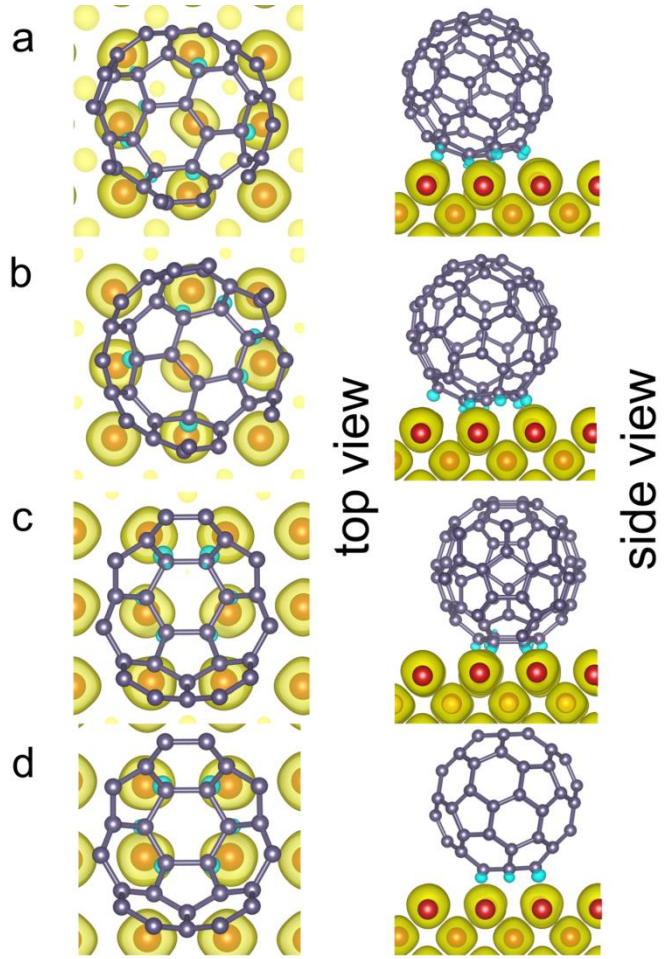

A.A. Kuzubov, E.A. Kovaleva, P.V. Avramov, A.S. Kholtobina, N.S. Mikhaleva, A.V. Kuklin, *Journal of Magnetism and Magnetic Materials*, 2016, **410**, 41-46.

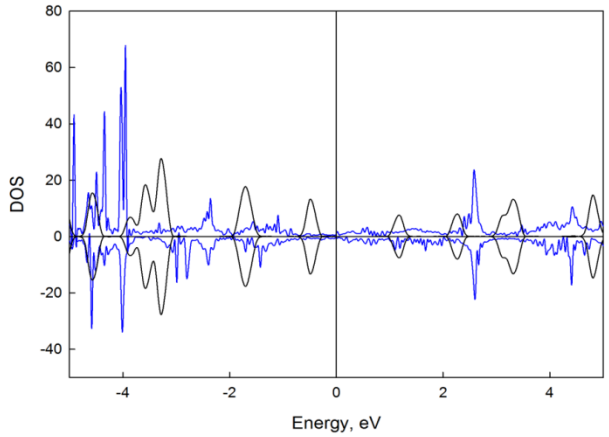

PDOS for C_{60} in bridge-2 composite (blue line) and DOS for the bare fullerene (black line)

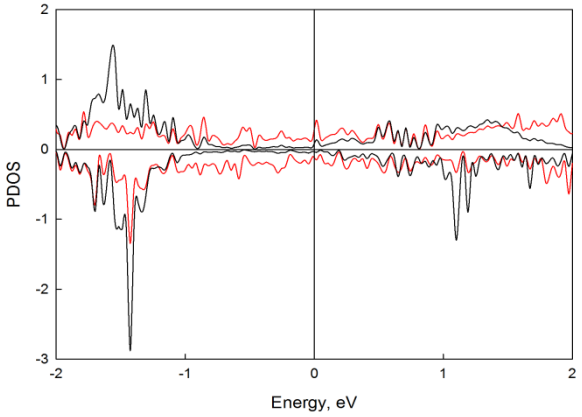

PDOS for carbon atoms in contact with substrate (red line) and atoms distant from the interface (black line)

C_{60}/Fe(001) composite configurations

$$P_i = \frac{e^{-\frac{E_i}{k_B T}}}{\sum_{i=1}^{N} e^{-\frac{E_i}{k_B T}}}$$

$$E_0 = \sum_{i=1}^{3N-3} \frac{h\nu_i}{2}$$

$$E_i^{\#} = \sum_{i=1}^{3N-4} \frac{h\nu_i^{\#}}{2}$$

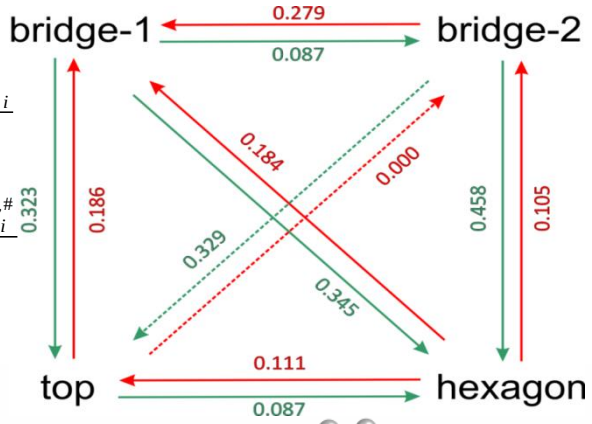

$$k = Ae^{-\frac{E_{barrier}}{kT}}$$

$$A = \frac{kT\prod_{i=1}^{3N-3}(1-e^{-\frac{h\nu_i}{kT}})}{h\prod_{i=1}^{3N-4}(1-e^{-\frac{h\nu_i^{\#}}{kT}})}$$

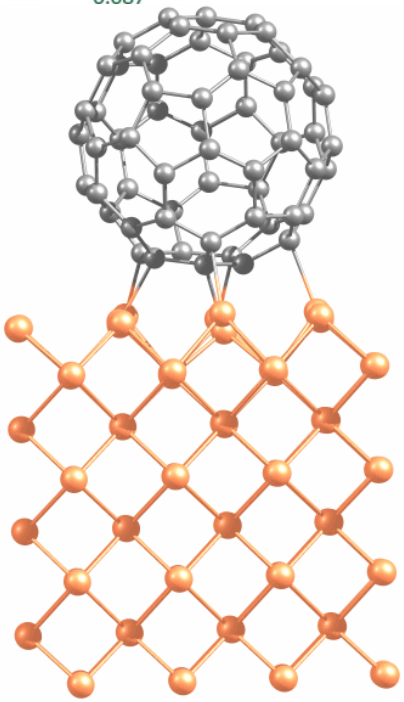

k =105410 s^{-1}

T = 300 K

P			
	Temperature, K		
	250	300	350
bridge-1	0.252	0.252	0.251
bridge-2	0.267	0.264	0.262
2C-bond	0.241	0.243	0.244
4C-atop	0.240	0.241	0.243

C_{60} averaged properties			
	Температура, K		
	250	300	350
Charge, e	1.982	1.980	1.980
Magnetic moment, μ_B	-0.119	-0.118	-0.118
Spin polarization at the Fermi level, %	-2.4	-2.5	-2.5

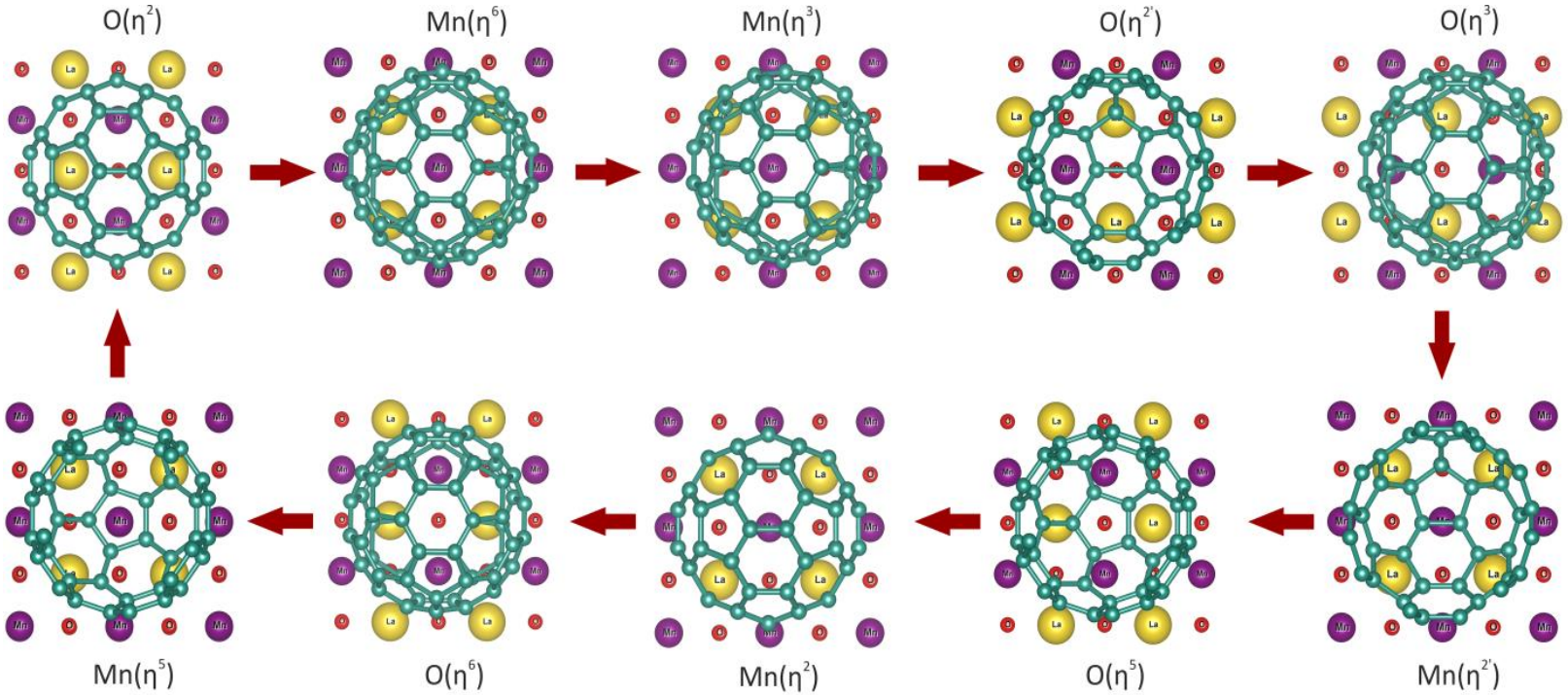

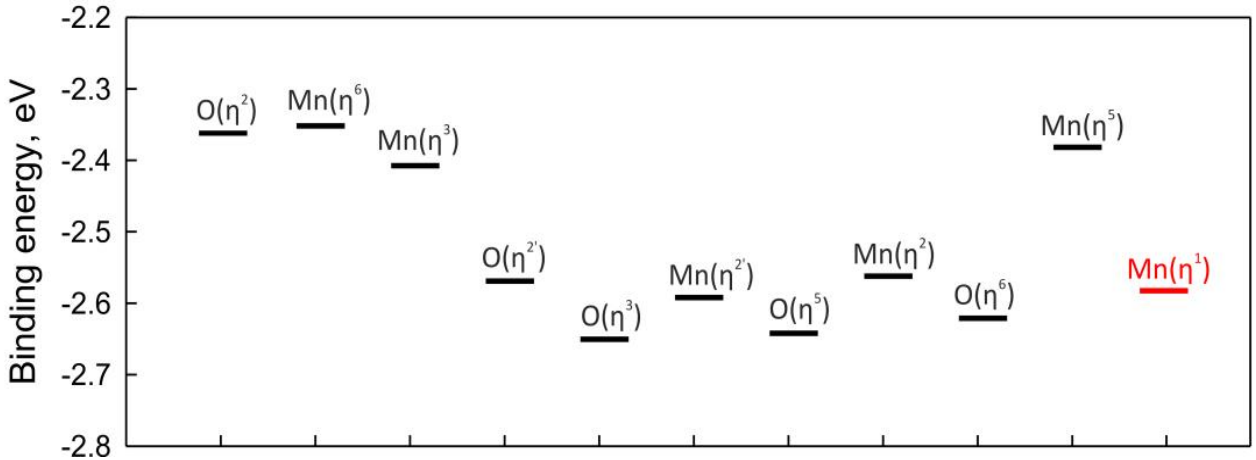

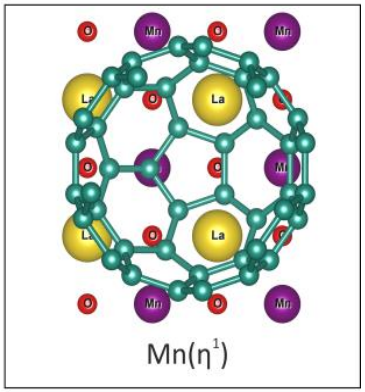

$$E_b = E_c - E_f - E_{LSMO},$$

E_c, E_f and E_{LSMO} are total energies of composite, fullerene and LSMO slab, respectively.

Probability (P) of each configuration appearance, averaged properties of C_{60} molecule

$$P_i = \frac{e^{-\frac{E_i}{k_B T}}}{\sum_{i=1}^{10} e^{-\frac{E_i}{k_B T}}}$$

P				
	Temperature, K			
	300	400	500	600
Mn(η^6)	less than 0.01	less than 0.01	less than 0.01	less than 0.01
Mn(η^5)	less than 0.01	less than 0.01	less than 0.01	less than 0.01
Mn(η^2)	0.01	0.03	0.04	0.06
Mn($\eta^{2'}$)	0.05	0.07	0.09	0.10
Mn(η^3)	less than 0.01	less than 0.01	less than 0.01	less than 0.01
O(η^6)	0.14	0.17	0.17	0.18
O(η^5)	0.32	0.30	0.29	0.27
O(η^2)	less than 0.01	less than 0.01	less than 0.01	less than 0.01
O($\eta^{2'}$)	0.02	0.03	0.05	0.06
O(η^3)	0.45	0.39	0.35	0.32

	Temperature, K			
	300	400	500	600
Charge, e	0.3677	0.3666	0.3658	0.3648
Magnetic moment, μB	0.0394	0.0398	0.0401	0.0403
Spin polarization at Fermi level, %	-18.6	-18.3	-18.0	-17.8

Spin density spatial analysis

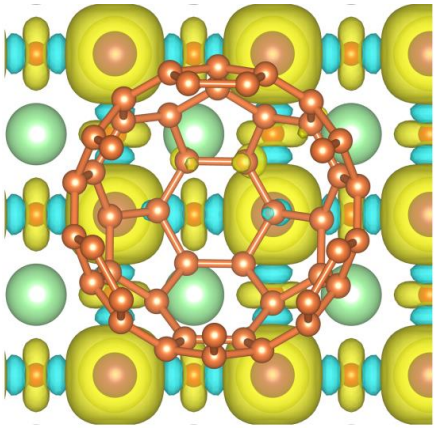

O(η^3) top view

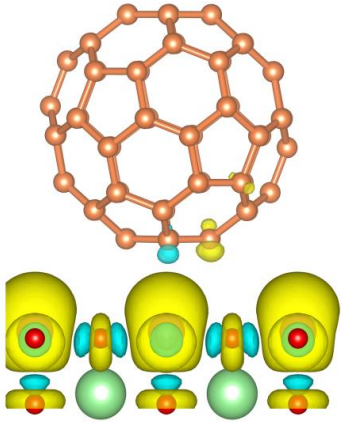

O(η^3) side view

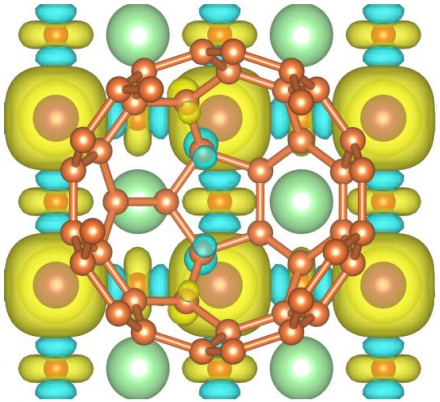

O(η^5) top view

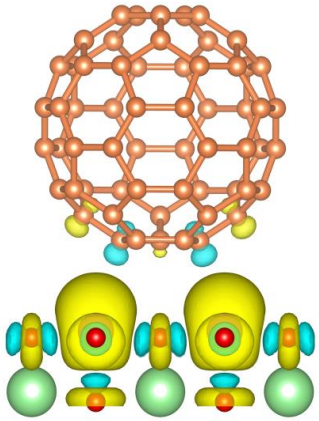

O(η^3) side view

- Charge of ~0.36 e
- Small value of magnetic moment (~0.04 μ_B)
- C upon Mn possess negative spin polarization
- Adjacent C atoms are positively spin-polarized

Additional Mn(η^1) configuration

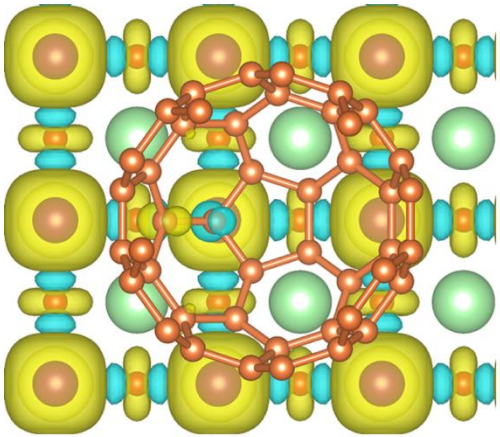

top view

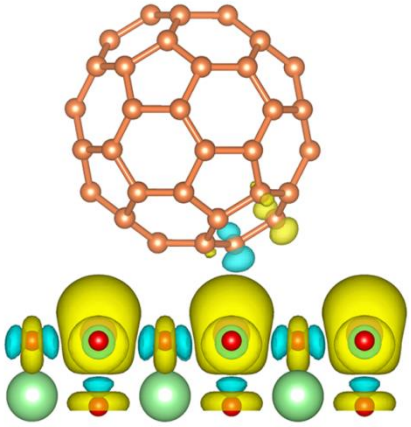

side view

- The same trend in spatial spin density distribution
- Only the minor difference between positively and negatively spin-polarized carbon atoms
- Mn affects contacting C atom making it negatively spin-polarized
- Contacting C, in turn, affects adjacent carbon atom resulting into positive spin polarization
- The overlapping between Mn orbitals and molecular orbitals of C_{60}

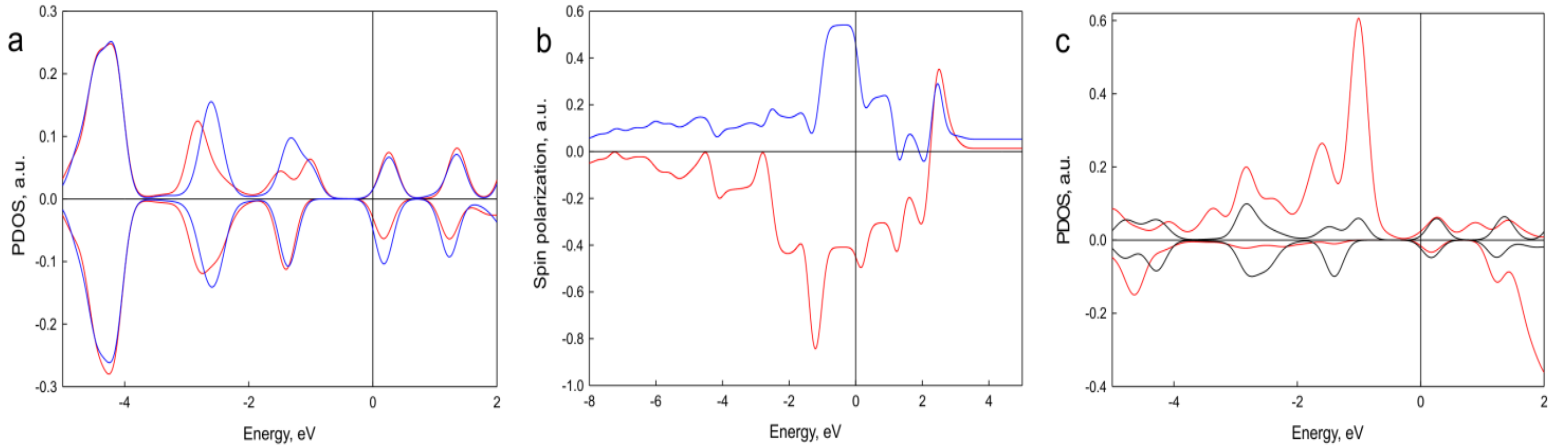

Partial density of states (a) and overall spin polarization (b) for C atom contacting with Mn (red line) and adjacent C atom (blue line); partial density of states (c) for Mn (red line) and carbon (black line) orbitals

Conclusions

- The interfaces of armchair and zigzag carbon and boron nitride nanotubes with ferromagnetic Co(0001) and Ni(111) surfaces was investigated by first-principles calculations. The electronic structure analysis reveals the presence of contact-induced spin polarization in all composites. It was found that NT(n,0)/Co composites are approximately twice as low in energy as NT(n,0)/Ni ones and spin polarization in these systems is also much stronger. Lower energy of CNT(9,0)/TM in comparison with CNT(10,0)/TM can be attributed to the difference in their conducting properties. Conducting nature of CNT(9,0) also causes a weaker spin polarization in comparison with other tubes. BNNTs demonstrate a local contact-induced conductivity while the fragments distant from interface remain to be insulating.
- Density functional study of atomic and electronic structure of C_{60}/Fe(100) and LSMO/C_{60} composites shows the coexistence of a number of possible structures with strong chemical bonding between iron slab snd fullerene molecule. Fullerene and slab deformation plays an important role in the formation of iron-based composites. Probabilities of configurations appearance were estimated according to the Gibbs distribution. Average charge transfer, magnetic moment on C_{60} molecule and its polarization at the Fermi level remain virtually the same within the range of 250 – 350 K.
- Manganese atoms play a key role in binding between carbon nanostructures and LSMO which is confirmed by the values of binding energies and spatial spin density distribution patterns. According to the analysis of magnetic moment values and spin density spatial distribution, it's evident that this is due to the special kind of magnetic ordering in C_{60} molecule and CNT(5,5) rising from the interaction with manganese atoms and complex magnetic exchange interaction.
- The interaction with LSMO(Sr-O) slab changes the electronic structure of the tubes noticeably. However, this change is mainly due to the deformation of the tubes, not the interaction with the substrate. The electronic structure of LSMO remains unchanged, and only a weak van-der-Waals interaction is responsible for the composite formation.

List of the articles published

1. Kuzubov, A.A. Contact-induced spin polarization in BNNT(CNT)/TM (TM=Co, Ni) nanocomposites / A.A. Kuzubov, **E.A. Kovaleva**, P. Avramov, A.V. Kuklin, N.S. Mikhaleva, F.N. Tomilin, S. Sakai, S. Entani, Y. Matsumoto, H. Naramoto // Journal of Applied Physics. - 2014. - Vol. 116. - 084309.
2. Kuzubov, A.A. On the possibility of contact-induced spin polarization in interfaces of armchair nanotubes with transition metal substrates / A.A. Kuzubov, **E.A. Kovaleva**, F.N. Tomilin, N.S. Mikhaleva, A.V. Kuklin // Journal of Magnetism and Magnetic Materials. - 2015. - Vol. 396. - P. 102–105.
3. Kuzubov, A.A. Buckminsterfullerene's movability on the Fe(001) surface / A.A. Kuzubov, **E.A. Kovaleva**, P.V. Avramov, A.S. Kholtobina, N.S. Mikhaleva, A.V. Kuklin // Journal of Magnetism and Magnetic Materials. – 2016. – Vol. 410. – P. 41-46.
4. **Kovaleva, E.A.** Characterization of LSMO/C_{60} spinterface by first-principle calculations / E.A. Kovaleva, A.A. Kuzubov, P.V. Avramov, A.V. Kuklin, N.S. Mikhaleva, P.O. Krasnov // Organic electronics. - 2016. - Vol. 37. - P. 55-60.

Interaction of CNT(9,0) and CNT(5,5) with Sr-O terminated LSMO surface

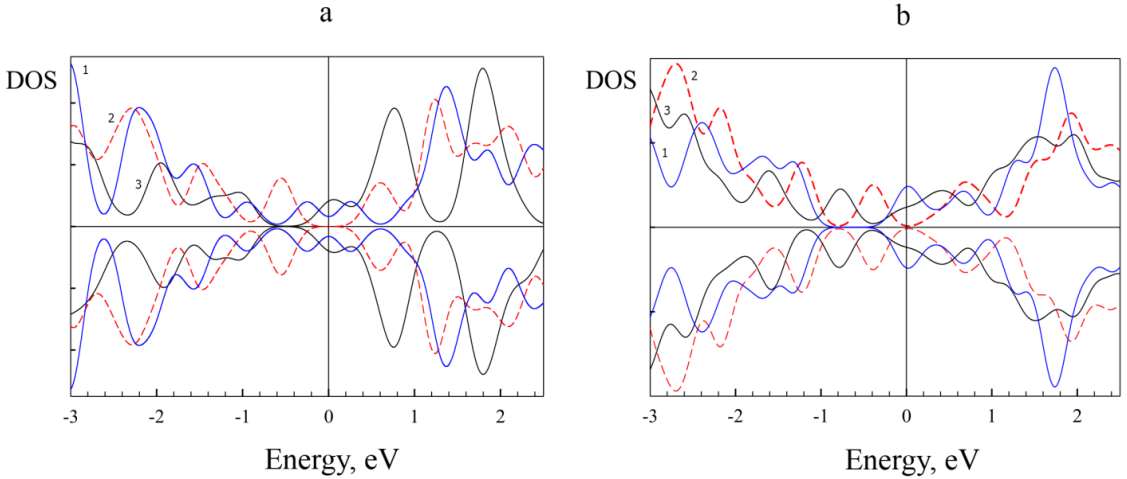

Densities of states for (a) CNT(5,5) and (b) CNT(9,0). Blue, red and black lines correspond to relaxed CNTs structures, strained CNTs structures with LSMO translation vector adopted, and partial densities of states of nanotubes in CNT/LSMO(Sr-O) composite.

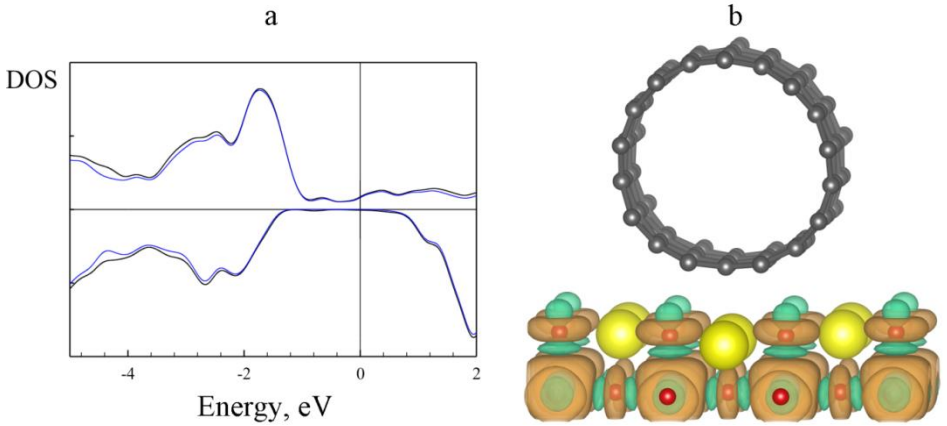

a) Density of states of CNT(9,0)/LSMO(Sr-O) heterostructure. Black and blue lines correspond to the total and partial LSMO DOS, respectively. b) Spatial distribution of spin density in CNT(5,5)/LSMO(Sr-O) heterostructure. Grey, yellow and red balls correspond to carbon, strontium and oxygen atoms; green and brown areas represent spin-up and spin-down density, respectively.

DFT-D3

- $E_{DFT-D3} = E_{KS-DFT} - E_{disp}$
- $E_{disp} = 1/2 \sum_{i=1}^{N_{at}} \sum_{j=1}^{N_{at}} \left(f_{d,6}(r_{ij}) \frac{C_6^{ij}}{r_{ij}^6} + f_{d,8}(r_{ij}) \frac{C_8^{ij}}{r_{ij}^8} \right)$
- $f_{d,n}(r_{ij}) = \frac{s_n}{1+6(r_{ij}/(s_{r,n}R_{0ij}))^{-\alpha_n}}$

NEB method

- $F_i^{NEB} = F_i^{\perp} + F_i^{S||}$
- $F_i^{\perp} = -\nabla(R_i) + \nabla(R_i) \cdot \hat{\tau}_i \hat{\tau}_i$
- $F_i^{S||} = k(|R_{i+1} - R_i| - |R_i - R_{i-1}|)\hat{\tau}_i \hat{\tau}_i$
- $F_i^{CI} = -\nabla(R_i) + 2\nabla(R_i) \cdot \hat{\tau}_i \hat{\tau}_i$

PAW method

- $|\psi_n\rangle = |\tilde{\psi}_n\rangle + \sum_i \left(|\phi_n\rangle - |\tilde{\phi}_n\rangle\right)\langle \tilde{p}_i|\tilde{\psi}_n\rangle$
- $\langle \tilde{p}_i|\tilde{\phi}_j\rangle = \delta_{ij}$
- $|\psi^{\mathrm{c}}\rangle = |\tilde{\psi}^{\mathrm{c}}\rangle + |\phi^{\mathrm{c}}\rangle - |\tilde{\phi}^{\mathrm{c}}\rangle$
- $|\psi_n\rangle$ and $|\tilde{\psi}_n\rangle$ - AE and PS wavefunctions
- $|\phi_n\rangle$ and $|\tilde{\phi}_n\rangle$ - partial AE and PS wavefunctions
- $\langle \tilde{p}_i|$ - projector function

DFT+U

- $E_{LDA+U}[\rho(r)] = E_{LDA}[\rho(r)] + E_{Hub}\left[\{n^{lq}_{mm'}\}\right] - E_{dc}[\{n^{lq}\}]$
- $E_{LDA+U}[\rho(r)] = E_{LDA}[\rho(r)] + \sum_I \left(\frac{U^I}{2}\sum_{m,\sigma\neq m'\sigma'} n^{I\sigma m} n^{I\sigma' m'} - \frac{U^I}{2} n^I (n^I - 1)\right)$
- $E_{dc}[\{n^l_{mm'}\}] = \sum_I \left\{\frac{U^l}{2} n^l (n^l - 1) - \frac{J^l}{2}\left[n^{l\uparrow}(n^{l\uparrow} - 1) + n^{l\downarrow}(n^{l\downarrow} - 1)\right]\right\}$